# Adaptation of machining toolpath to distorted geometries: application to remove a constant thickness on rough casting prosthesis

Noureddine Azzam, Julien Chaves-Jacob, Salim Boukebbab, Jean-Marc Linares

# Adaptation of machining toolpath to distorted geometries: application to remove a constant thickness on rough casting prosthesis

Noureddine Azzam & Julien Chaves-Jacob & Salim Boukebbab & Jean-Marc Linares

Abstract This study proposes a method to adapt the geometry of the toolpath to a specified target. In the case study presented, the geometrical target is to remove a constant thickness on the rough workpiece. This case is normally present in the polishing of the femoral component of knee prostheses. In fact, an operator carries out these operations manually. The aim of this study is to contribute to the automation of prosthesis production, notably, in the preparation of surface polishing. The proposed method can deform and adapt a toolpath to ensure the required geometry of the machined surface. The proposed toolpath deformation method is composed of three steps: alignment, toolpath deformation, and toolpath smoothing. Alignment between the measured surface of the roughcast prostheses and the nominal toolpath is carried out by an Iterative Closest Point (ICP) algorithm. The principle of this algorithm is to find the optimal rigid transformation to readjust the toolpath on the measured surface. Subsequently, the toolpath is deformed to remove the constant thickness of the roughcast prostheses. Next, to increase the machined quality, a smoothing stage is carried out on the obtained toolpath. Experimental tests on industrial prostheses geometry are conducted to validate the effectiveness of this method.

N. Azzam
Department of Mechanical Engineering, Faculty of Sciences and Technology, University of Constantine 1, Ain-el-Bey Road, 25000 Constantine, Algeria

N. Azzam · J. Chaves-Jacob (✉) · J.<M. Linares
Aix-Marseille Université, CNRS, ISM UMR 7287, 13288 Marseille cedex 09, France
e-mail: julien.chaves-jacob@univ-amu.fr

S. Boukebbab
Department of Engineering Transport, Faculty of Sciences and Technology, University of Constantine 1, Ain-el-Bey Road, 25000 Constantine, Algeria

Keywords Toolpath adaptation · Biomanufacturing · ICP algorithm · Five-axis machining · Toolpath smoothing

## 1 Introduction

The United Nations said, "The rapid ageing of the world's population is one of humanity's greatest triumphs. It is also one of our greatest challenges for the future. Global ageing will put increased economic and social demands on all countries. At the same time, older people are a precious, often ignored, resource that makes an important contribution to the fabric of our societies." The United Nations study predicts that in 15 years, the number of older people will have doubled in comparison to the year 2002. For the elderly, osteoarthritis is a common problem; this illness reduces their functional capacity. To increase their functional capacity, the surgeon proposes to change their biological joint with an artificial prosthesis. However, the service life and cost of the knee prosthesis are considered as not acceptable by the health care and social security systems. Today, the mean value of its service life is 10 years. Nowadays, research work aims to increase the knee prosthesis service life to 15 years and to reduce its manufacturing costs. The challenge of our work is to reduce the production cost and avoid operator health problems in the production of prosthesis [1]. These objectives are obtained thanks to automation in the manufacturing stage. The presented work proposes a method to adapt toolpath to manufacturing prostheses by a machine.

Generally, knee prostheses are composed of three elements, as presented in Fig. 1. Two metal parts fixed on the femur and the tibia and a third part composed of high-density polyethylene material. The most complex part is the femoral workpiece. This component is thin in order to reduce the removed bone volume. Furthermore, it is submitted to a high level of stress. Accordingly, control of the femoral component thickness is

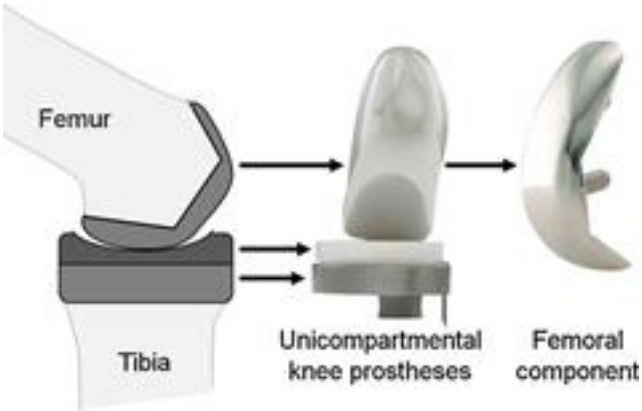


Fig. 1 Knee prostheses components

one of the main problems. On the other hand, the geometry form of this type of component does not need high accuracy. As illustrated in Fig. 1, the contact between the femoral component and the polyethylene workpiece is nonconforming. This property induces contact stability for small geometrical variations. Accordingly, the main geometrical constraint on the femoral prosthesis is to ensure the specified thickness. Consequently, the surface form is not critical. Furthermore, the movement amplitude between these two components can induce a wear risk. To limit this risk, a high roughness quality (mirror effect) is required on the femoral component. To summarize, the two main functional characteristics of a femoral component are ensuring the nominal thickness and the roughness.

The femoral component manufacturing process is presented in Fig. 2. This component is generally manufactured in a cobalt-chrome alloy, which has good tribological properties but poor machinability. The CAD model specifies the kinematic and functional requirements. Next, the rough of prostheses is obtained by lost-wax casting. Before beginning the polishing stages, rough and semifinishing machining operations are carried out on a milling machine. The polishing stage is carried out with a succession of abrasive tools. For finishing, the prosthesis undergoes numerous cleaning and sterilization procedures. During the casting process, the geometry of the rough workpiece changes due to structural deformations. To facilitate manufacture of the workpiece, casting allowances for machining are reduced to a minimal.

Figure 3 illustrates a workpiece deformed during the casting process. As previously shown, the final implant geometry is not crucial for prosthesis functionality. Consequently, manufacturers select to remove a constant thickness relative to the real rough surface. This choice ensures the mechanical strength maintaining the nominal prosthesis thickness. Manually, the operator instinctively adapts the polishing toolpath to ensure an adequate polishing force. On the other hand, the usual CNC machine is driven in

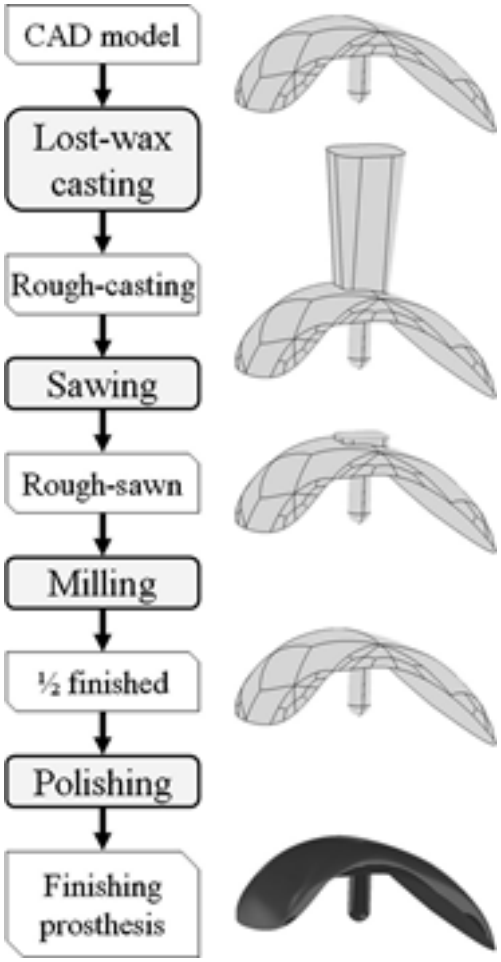


Fig. 2 Process planning of a knee prosthesis femoral part

position and not in force by the numerical controller. This imposes the geometrical adaptation of the machining toolpath at each rough workpiece. The toolpath deformation step must be applied at each stage of the prosthesis process planning: rough and semifinishing milling. Furthermore, if a CNC machine is used to carry out the

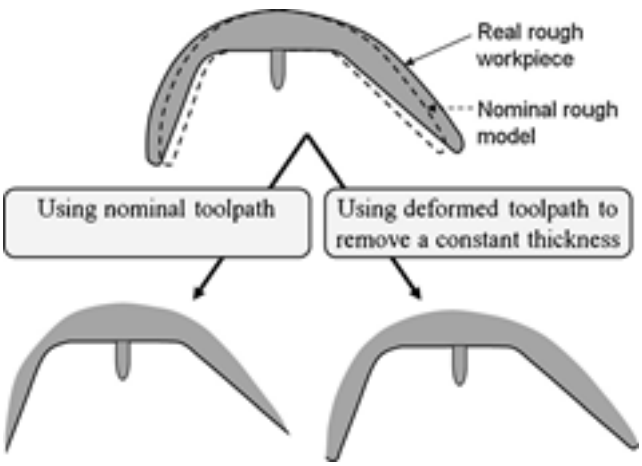


Fig. 3 Toolpaths impact on the final prostheses thickness

polishing step [2], its polishing toolpath must also be deformed. Certainly, like a human, the machine needs eyes to capture the rough geometry. The proposed method requires a 3D measurement of the rough workpiece. Figure 4 illustrates the measurement process on an optical coordinate measuring machine to carry out the rough surface measure. After this process, a stereolithography (STL) model is generated. The proposed method adapts the nominal toolpath to the measured real surface.

This study is composed of six sections. Firstly, a state of the art is carried. The second section details the method used to align the measured surface on the nominal toolpath. This method is based on the Iterative Closest Point (ICP) algorithm. Next, the deformation procedure is presented. After this deformation step, a smoothing stage is used to increase the obtained surface quality. The fifth section presents the overall procedure to treat a toolpath; this section presents the iterative procedure to obtain the final toolpath. Finally, the last section proposes a machining test, which validates the usefulness of the method on an industrial workpiece: a friction surface of femoral knee prosthesis.

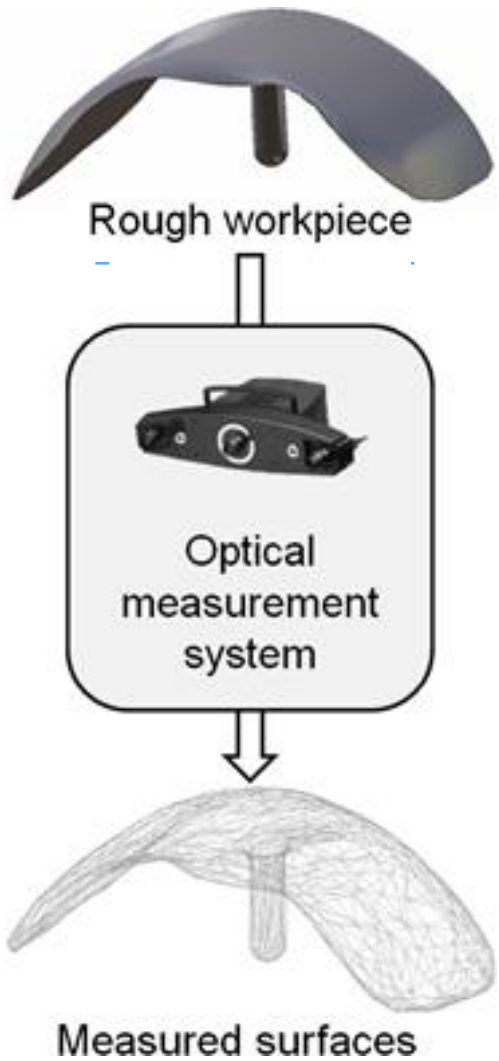

Fig. 4 Measurement of the rough surface geometry

## 2 State of the art

This study proposes a method to adapt the geometry of the toolpath to a specified target. In the case study, the geometrical target is to remove a constant thickness compared to the measured real rough surface. As presented in the introduction, this case is present in the production process of the femoral component of knee prostheses. The proposed method can deform a toolpath to ensure the required geometry of the machined surface. Figure 5 illustrates the stages of this method. The proposed toolpath deformation method is composed of three stages: the measured surface alignment, toolpath deformation, and toolpath smoothing. Each of these three items is studied in relation to the bibliography.

Alignment is carried out between the nominal toolpath defined by a succession of points and the measured rough surface defined by an STL file. An STL file is composed of triangular facets. Each facet has three edges and vertices. The alignment procedure is carried out with an ICP algorithm. The ICP algorithm is a well-known method for registering a 3D set of points to a 3D model [3]. Since the presentation of the ICP algorithm by Besl et al. [4], many variants have been introduced [5–7]. New propositions affect one or more stages of the original algorithm to try to increase its performance, especially accuracy and speed. The ICP algorithm minimizes the sum of squared residual errors between the set of points and the model [4]. Its main goal is to find the optimal rigid transformation, which will match a set of measured points suitably to a geometrical model. The algorithm requires a fine initial estimation because the computation speed and best-fit accuracy depend on how this initial estimate is chosen [8]. In this algorithm, the 6 degrees of freedom are defined by three rotations and three translations. While the 3D translation vector simply has three parameters, the rotation matrix is composed of nine elements which correspond to the six conditions for orthonormality. In the case of a first-order series expansion of transformation matrix, a simple iterative optimization based on the least square principle cannot guarantee this orthonormality [9]. Consequently, improved ICP employs unit quaternion to represent the 3D rotation parameters in order to reduce this problem [10]. The total error of alignment is composed of two types of errors; the first is given by the algorithm iteration and the second results from the STL model meshing.

Toolpath deformation is carried out to adapt the geometry of the machined or polished surface. Smith et al. [11] propose a hybrid process, a mix of machining of thin wall structures and single-point incremental forming. The authors voluntarily

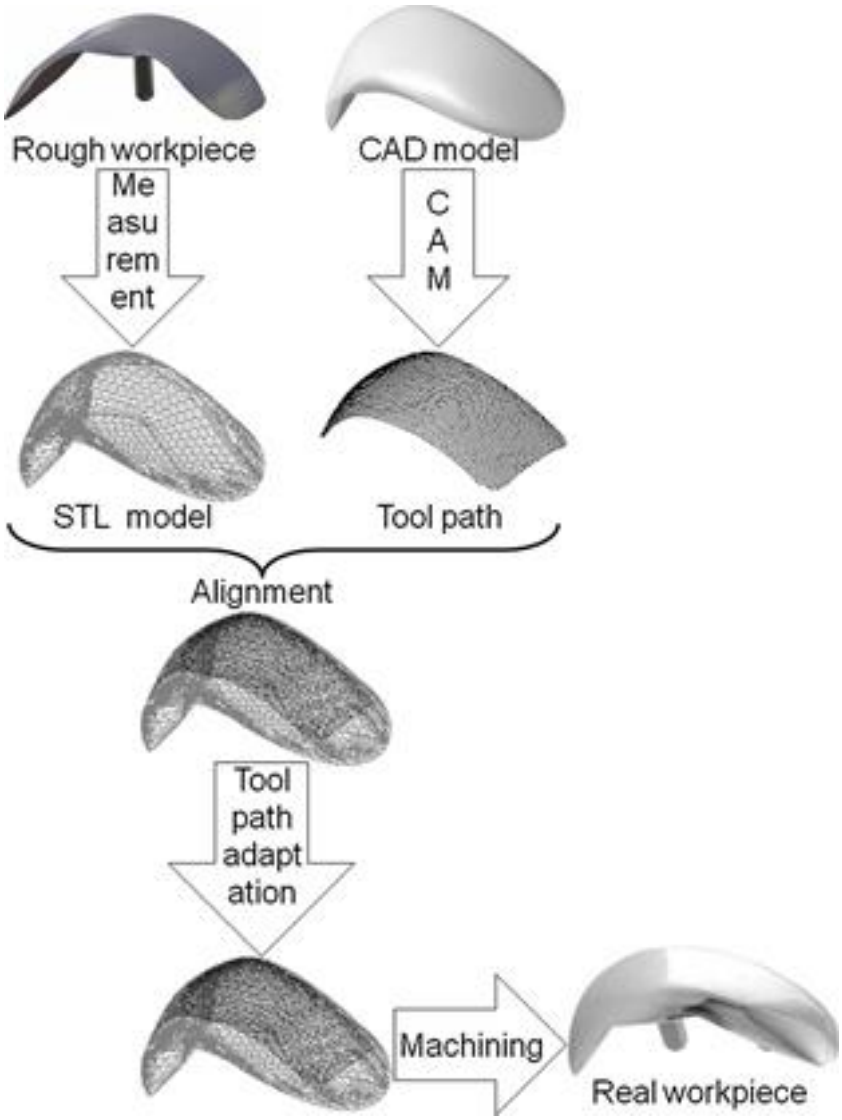


Fig. 5 Toolpath adaptation method steps

deform the toolpath to twist the thin wall to obtain the desired geometry. The idea in this paper is not really to adapt the toolpath but to deform the workpiece. Other works such as those presented by Redonnet et al. [12] or Menzel et al. [13] propose adapting the toolpath to optimize the machining of undevelopable ruled surfaces. Belchior et al. [14] propose a method to adapt the toolpath of an industrial robot taking its deformation into account. Certainly, industrial robots are more flexible than milling machines. In this study, the author proposes a prediction of the robot deformation and adapts the toolpath to obtain the desired geometry. Biermann et al. [15] also present a toolpath adaptation method to compensate tool flexion in micro-milling machining. Moreover, the author proposes to use the control point of B-spline curves to adapt the toolpath to balance the tool flexion. Wan et al. [16] propose a method to adapt the toolpath of the thin wall workpiece deformation. All these studies propose to adapt the toolpath to compensate environment errors, but the geometrical target is still the nominal surface. On the other hand, Béarée et al. [17] propose a method for the deburring process of aeronautical structure by an industrial robot. In this paper, the authors compensate the aircraft structure deformation.

Toolpath smoothing is carried out to improve toolpath quality after the deformation stage. Certainly, during the deformation step, a meshed surface is used, inducing discontinuities of the deformed toolpath. Smoothing methods have been developed in literature. The authors propose B-spline curve interpolation to smooth the trajectory between the nominal toolpath points. Lartigue et al. [18] proposed this solution and experimentally demonstrate the usefulness of this method to decrease surface faceting. These methods are efficient in smoothing the toolpath computed on a smooth model but are not powerful enough when the initial toolpath is too rugged. As presented in this case study, the initial toolpath points must be moved.

## 3 Alignment process by ICP algorithm

In this application case, the geometrical target is to remove a constant thickness compared to the measured rough surface. Firstly, the measured rough surface must be aligned on the nominal toolpath. The toolpath is composed of the successive coordinates of the drive point expressed in the workpiece coordinate system. Some CAM software options allow expression of the toolpath of the cutter contact point. Subsequently, these coordinates were noted $P_{CCi}$ and the tool axis direction, u. On the other hand, an STL file defines the measured surface. The STL model is composed of vertices, edges, and triangular facets. Each facet has a normal vector, n. The ICP algorithm was used to best fit the measured rough surface on the nominal toolpath. The orthogonal projection of $P_{CCi}$ on a triangular facet of an STL model is noted $P'_{CCi}$. A rigid transformation $T_t$, is computed to displace the measured surface on the nominal surface. As presented in Eq. 1, this transformation is composed by a rotation matrix [R] and a translation vector {T}.

$$OP'_{CCi} = [R]\,OP_{CCi} + \{T\} \quad (1)$$

The ICP algorithm can be summarized as follows:

- Input data; toolpath $P_{CCi}$ and measured surface (STL file),
- Computation of the toolpath projection on the measured surface (computation of $P'_{CCi}$),
- Calculation of the best rigid transformation $T_t$, to associate $P_{CCi}$ at $P'_{CCi}$, this stage is carried out using a singular value decomposition method,
- Transformation $T_t$, is applied to $P_{CCi}$,
- Evaluation of residues,
- If residues are lower than a specified value or if the maximum number of iterations is attained, the iteration is stopped, otherwise the iteration continues.

The transformation is calculated to displace the toolpath on the measured surface. Next, the inverse transformation is applied to the measured surface. This operation avoids the displacement of the toolpath relatively to the workpiece framework. Accordingly, the toolpath is still expressed in the same framework.

## 4 Deformation and offset of the toolpath

Section 3 illustrates the best-fit method between the nominal toolpath (points $P_{CCi}$) and the measured surface (defined by an STL file). Once this operation is completed, the toolpath is deformed to carry out the required geometry. In this study, the presented geometric target is to remove a constant thickness (noted $a_p$ in Fig. 6) compared to the displaced rough surface. Naturally, the procedure can be applied to any other geometrical target. Consequently, the aligned toolpath is deformed in two steps. The first step is the projection of the aligned points on the measured surface. In the second step, these points are offset by a value ($a_p$) to obtain the required geometry. These steps are detailed below.

### 4.1 Projection step

An STL file defines the measured surface. Firstly, all the points of the trajectory $P_{CCi}$ are projected on all facets of the measured STL surface. Subsequently, a test is carried out to discern if the projection is inside the triangle. Once this test is conducted, three situations may occur:

- Only one projection point is inside a triangle, so its projection is denoted $P_{CCi\_def}$;
- No projection points are inside any triangles, so $P_{CCi}$ becomes $P_{CCi\_def}$;
- More than one projection point is inside several triangles, so only the point having the minimum distance with $P_{CCi}$ is kept and becomes $P_{CCi\_def}$.

The calculation of the distance between $P_{CCi}$ and a triangular of the STL model is carried out using Eq. 2. The triangle vertices are denoted $N_1$, $N_2$, and $N_3$. Equation 3 is used to calculate the point $P_{CCi\_def}$.

$$d_i = P_{CCi}N_1 \cdot n \quad (2)$$

$$OP_{CCi\_def} = OP_{CCi} + d_i \cdot n \quad (3)$$

where n is the unit vector of the normal to the triangle, it is provided in the STL model and $d_i$ is the distance between $P_{CCi}$ and $P_{CCi\_def}$.

### 4.2 Offsetting the toolpath

In this paper, the geometrical target selected is to remove a constant thickness of material on the rough surface. For this, the projected toolpath (points $P_{CCi\_def}$) is offset inside material with a quantity $a_p$: depth of cut to achieve the points ($P_{CCi\_def\_dec}$). Equation 4 is used to carry out this calculation.

$$OP_{CCi\_def\_dec} = OP_{CCi} + \frac{d_i - a_p}{\cdot} \cdot n \quad (4)$$

where n is the unit normal vector for the facet, $a_p$ is the depth of cut, and $d_i$ distance between $P_{CCi}$ and $P_{CCi}$. $P_{CCi\_def\_dec}$ are contact points between the tool and the desired surface.

After $P_{CLi\_def}$, the driven point is computed as presented in Fig. 7. Tool axis is noted u. Relationship between the contact points $P_{CCi\_def\_dec}$ and the drive points $P_{CLi\_def}$ depends on the

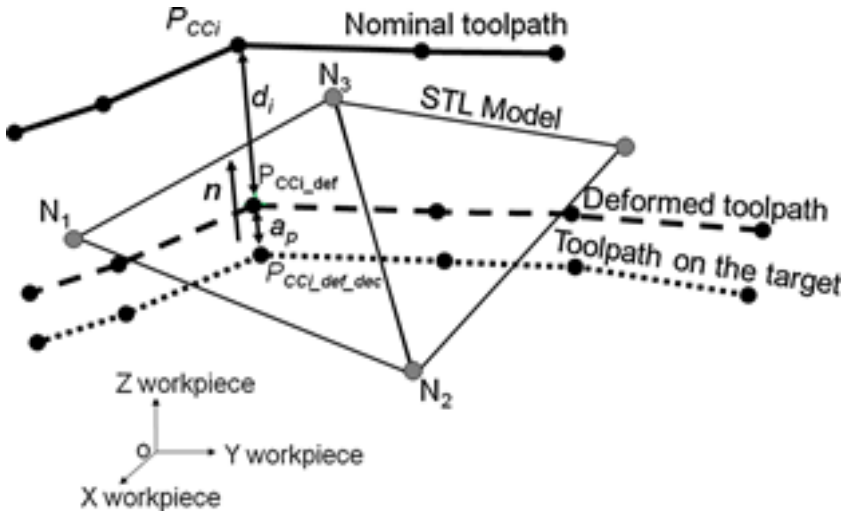


Fig. 6 Deformation of the nominal toolpath

geometry of the tool [19, 20]. In the case of the ball end tool, Eq. 5 can achieve the calculation.

$$OP_{CLi\_def} = OP_{CCi\_def\_dec} + r \cdot (n - u) \quad (5)$$

where r is the radius of the tool, n is the unit vector of surface normal, and u is the unit vector of the tool axis.

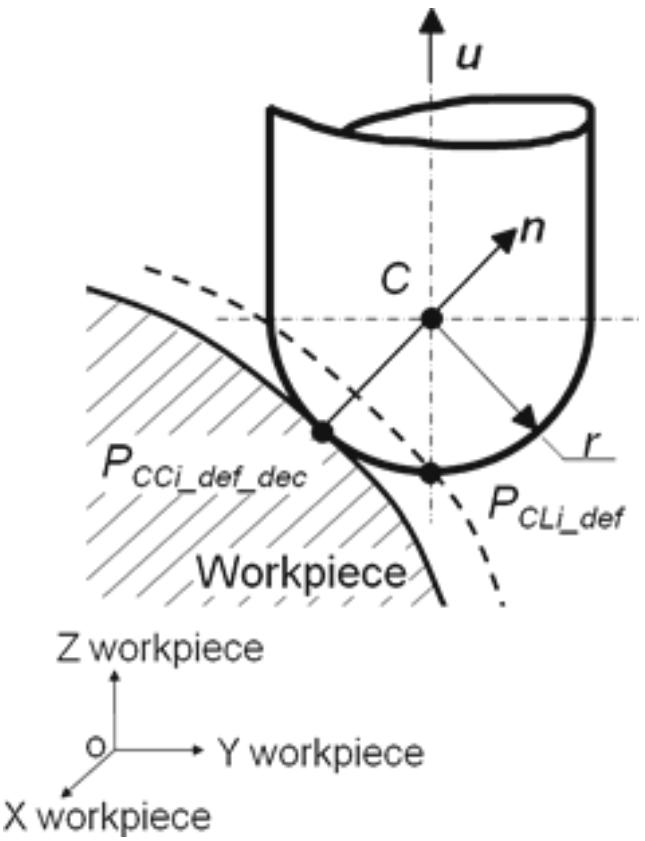


Fig. 7 Tool positioning in the part coordinate system

The toolpath obtained with this method ensures the desired geometry (e.g., removing a constant thickness of the part). To deform the trajectory, a meshed model is used. This model is composed of triangles with different normal. Consequently, on a meshed surface the local normal is submitted at discontinuous variations along a toolpath. Subsequently, during the toolpath deformation step, the meshed surface normal is used (Eqs. 2 to 5). This will induce discontinuities on the deformed toolpath. Figure 8 illustrates this problem. To control this problem, Section 5 proposes a method to smooth the toolpath.

## 5 Toolpath smoothing method

The proposed method carries out smoothing of the toolpath ensuring a control of the gap between the initial and the smoothed toolpath. Firstly, elemental paths are detected. Naturally, point milling of free-form surfaces are obtained by numerous juxtaposed paths. These paths are identified by their input and output points. The input and output movements are generated by the machining strategy. Subsequently, a smoothing method is carried out on the elementary path. This method is based on smoothing axis by axis with a 3D admissible tolerance IT. This method may be applied to the three axes of the toolpath or only to one. On each axis, a low degree polynomial (<6) is calculated using the least squares method. In our example, a polynomial of 5° is used. Equation 6 shows the form of the polynomial.

$$P_{Li}(t) = \begin{cases} a_0 + a_1 t + a_2 t^2 + a_3 t^3 + a_4 t^4 + a_5 t^5 \\ b_0 + b_1 t + b_2 t^2 + b_3 t^3 + b_4 t^4 + b_5 t^5 \\ c_0 + c_1 t + c_2 t^2 + c_3 t^3 + c_4 t^4 + c_5 t^5 \end{cases} \quad (6)$$

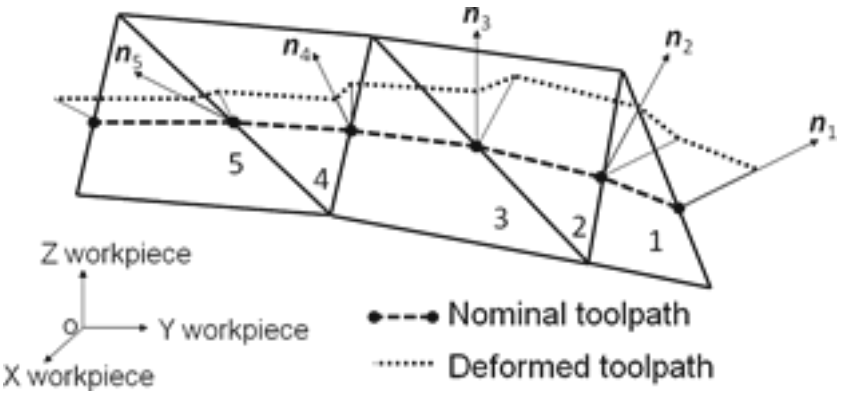


Fig. 8 Discontinuities of the deformed toolpath

Subsequently, the gap $E_i$ between the initial toolpath and the polynomial smoothing point is computed using Eqs. 7 and 8.

$$\begin{cases} ex_i = OP_{CCi\_def\_dec}.X - a_0 + a_1 t + a_2 t^2 + a_3 t^3 + a_4 t^4 + a_5 t^5 \\ ey_i = OP_{CCi\_def\_dec}.Y - b_0 + b_1 t + b_2 t^2 + b_3 t^3 + b_4 t^4 + b_5 t^5 \\ ez_i = OP_{CCi\_def\_dec}.Z - c_0 + c_1 t + c_2 t^2 + c_3 t^3 + c_4 t^4 + c_5 t^5 \end{cases} \quad (7)$$

$$E_i = \sqrt{ex_i^2 + ey_i^2 + ez_i^2} \quad (8)$$

Figure 9 and Eq. 9 present both possible smoothing cases:

- Case 1: $E_i < IT$; the point of the initial trajectory, $P_{CCi\_def\_dec}$, is replaced by the point of the polynomial curve, $P_{Li}$.
- Case 2: $E_i > IT$; the point of the initial trajectory is moved nearer to the polynomial curve. This displacement has an IT value.

$$\begin{cases} \text{Case1; } E_i < IT : \overrightarrow{OP_{CCi\_def\_dec}} \leftarrow \overrightarrow{OP_{Li}} \\ \text{Case2; } E_i > IT : \overrightarrow{OP_{CCi\_def\_dec}} \leftarrow \overrightarrow{OP_{CCi\_def\_dec}} + IT \cdot \dfrac{\overrightarrow{P_{CCi\_def\_dec}P_{Li}}}{\left\| \overrightarrow{P_{CCi\_def\_dec}P_{Li}} \right\|} \end{cases} \quad (9)$$

This smoothing method guarantees a maximal gap with the initial toolpath.

## 6 Deformation and smoothing process of a toolpath

In the overall toolpath treatment process, the deforming (Section 4) and smoothing (Section 5) methods are used iteratively in three steps. Consequently, the first iteration begins with the deformation of the initial trajectory. This deformation induces numerous oscillations because the initial trajectory is far from the target surface, accordingly, deformation will be significant. Subsequently, the smoothing method is carried out with a large tolerance. This smoothing step will be very efficient but will induce a large deviation of the toolpath to the geometrical target. The second iteration deforms the toolpath again to stick to the target geometry. The generated displacements at this iteration are smaller than those in the first iteration. Next, a new smoothing step is conducted with a reduced tolerance. The third iteration begins with the toolpath sticking to the target geometry. This step is followed by a smoothing stage with a tight tolerance (less than allowed by the form defect).

## 7 Experimental validations

Tests are carried out on a friction surface of a femoral prosthesis. This prosthesis is a unicompartmental knee component. The shape complexity of these surfaces imposes the use of a multi-axis CNC machine. Accordingly, a 5-axis "ULTRASONIC 20 linear" machine tool with a Siemens 840D CNC was used to carry out the tests. Figures 10 and 11 show the test piece manufactured in machinable resin, PROLAB 65. Tests were carried out with the following cutting conditions: lubrication: carbide ball end tool of diameter $D=10$ mm, 4 flutes, rotation speed of $N=15{,}000$ rpm, feed rate of $V_f=3{,}000$ mm/min, and depth of cut $a_p=0.2$ mm. The machining process is divided into two operations: roughing and finishing. The aim of the roughing stage is to reproduce a surface, which may be obtained by cast process. Procedures of toolpath deformation are only applied for the finishing operation. The initial machining trajectories were generated using a strategy in iso-planar with a feed rate in Y direction. The chordal tolerance used to compute the finishing toolpath was 0.03 mm. Figure 10 illustrates the workpiece after the roughing stage. Furthermore, this figure presents the position of the nominal surface (used to compute the initial toolpath) between the rough workpiece. Likewise, this figure highlights the maximum and minimum gap values (0.582 and 0.109 mm) between the rough and nominal surfaces for a line.

### 7.1 Validation of toolpath deformation

Two toolpaths are used: the nominal toolpath and the deformed toolpath to remove a constant thickness against

Fig. 9 Smoothing method

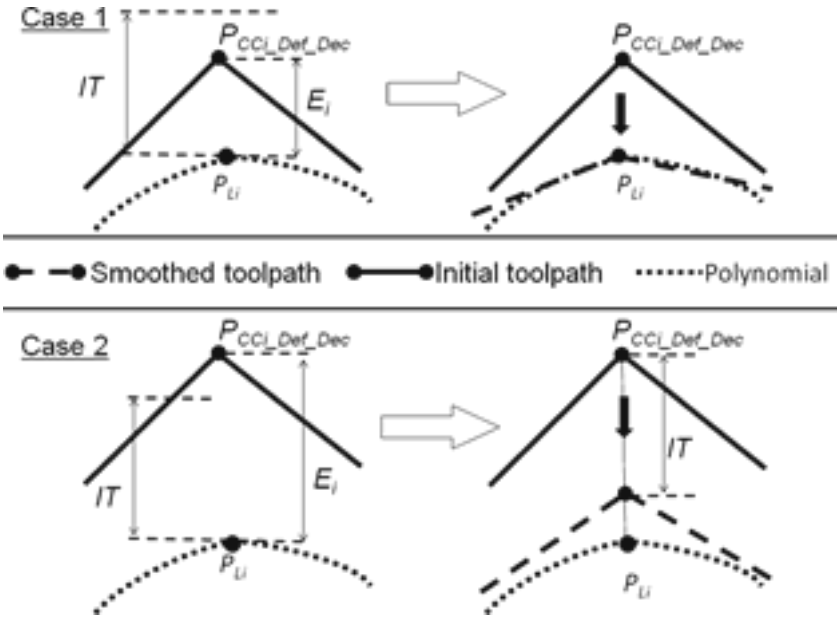


the rough surface. No smoothing methods are used in this experiment. Note that the rough surface was accurately measured (around 0.05 mm) using an optical measurement. Accordingly, this surface is defined by a meshed CAD model (STL). Figure 11 shows the part created during this test.

Subsequently, machined surfaces are measured with the optical coordinate measuring machine. Figure 12 presents the obtained results. This figure illustrates the interference cartography between the machined surface and the target surface (roughed surface offset inside the material of 0.5 mm). This figure highlights the machining interferences (overcut and undercut) induced by the nominal toolpath as between −0.5 and 0.1 mm. On the other hand, those caused by the deformed toolpath are between −0.06 and 0.02 mm. This study demonstrates that the proposed deformation method is efficient. Visually, in this experimental test, the STL patterns appear on the machined surface.

## 7.2 Validation of toolpath smoothing

The aim of this section is to validate the usefulness of the methods presented in Section 4. The same cutting conditions and protocol as in Section 7.1 are used. Two different toolpaths are used to conduct the finishing step. Both toolpaths are deformed and smoothed three times with successive smoothing tolerances 0.04, 0.03, and 0.02 mm (see Section 6). The first toolpath is smoothed along the three axes, while the second is only smoothed along the X axis. This direction is of the iso-

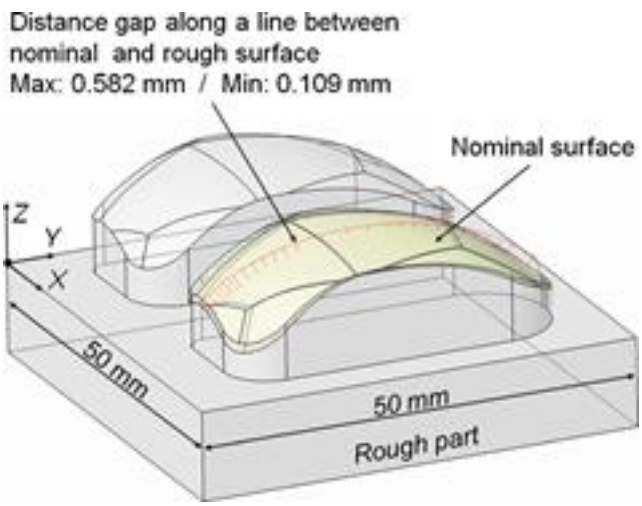


Fig. 10 Gap between the nominal and rough surfaces

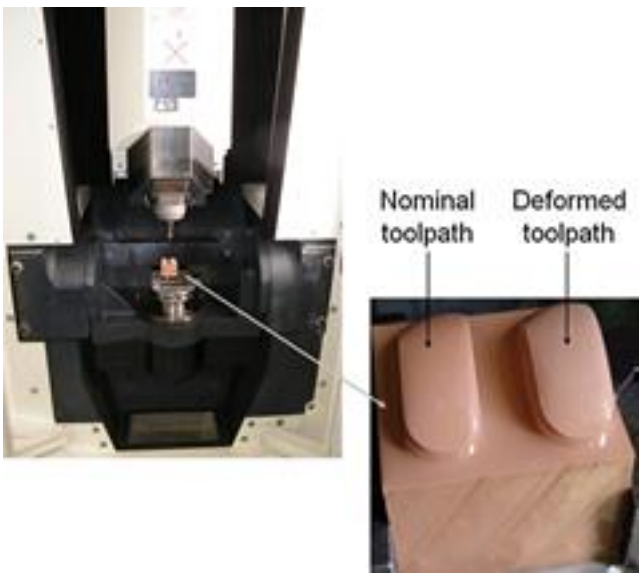


Fig. 11 Experimental part

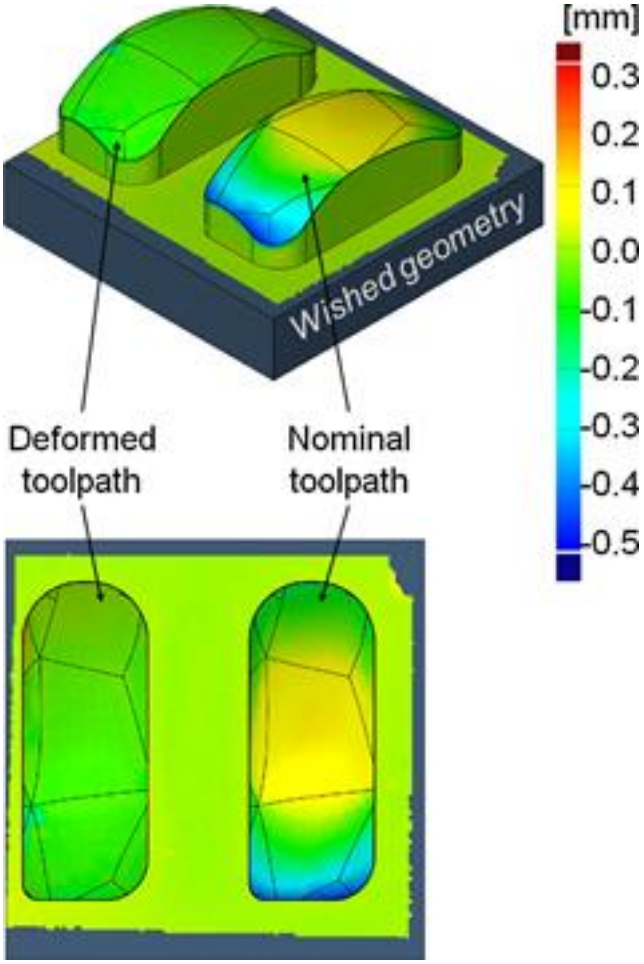


Fig. 12 Comparison between the nominal and the deformed toolpath interferences

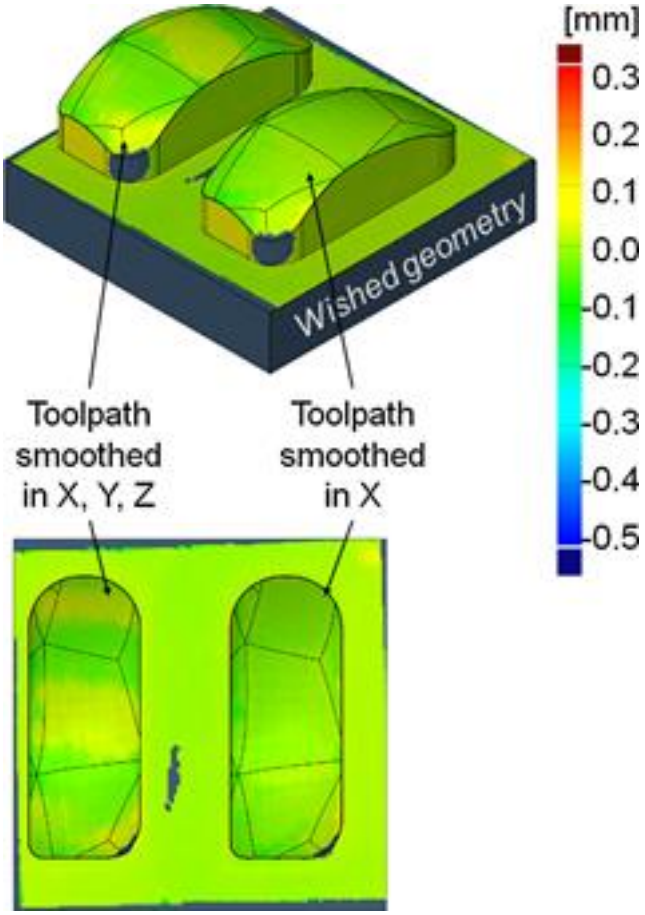


Fig. 13 Smoothing effect in one or three directions

planar strategy. In this direction, the initial path has a constant value along an elementary path.

Figure 13 presents the interference cartography between the machined surfaces and the target surface. This figure highlights a higher interference for the toolpath smoothed in the three axes. These interferences may be explained by the additional smoothing in three directions of the toolpath. Certainly, smoothing in three directions uses all the accepted tolerance values for smoothing, whereas the other case does not use all the tolerance values.

As mentioned, the mesh pattern appears visually on the machined surface with the deformed toolpath. In the selected case, the target geometry is defined by a meshed surface (machine a uniform thickness against a measured surface). Consequently, the meshed surface is used to deform the nominal toolpath.

### 7.3 The impact of mesh refinement on the machined surface quality

This section studies the influence of the mesh model refinement on the machined surface quality. Figure 14 shows the two used meshed surfaces noted STL1 and STL2. STL1 is the meshed surface used to conduct the tests in Sections 7.1 and 7.2. This meshed surface has an average step of 5 mm and a chordal error of 0.05 mm. STL2 is a much finer meshed surface (average step 2 mm and chordal error of 0.005 mm).

Figure 15 shows the measured interferences against the geometrical target and the machined surface with three strategies. Toolpaths are smoothed (successive tolerances of smoothing 0.04, 0.03, and 0.02 mm) and deformed using the following:

- STL1 model with a smoothing of the path on the three axes,
- STL1 model with a smoothing of the path on the X axis alone,
- STL2 model with a smoothing of the path on the X axis alone.

Manufacturing parameters are the same as those used in Section 7.1. The tolerance scale of Fig. 15 was tightened to −0.08/0.08 mm compared to Figs. 12 and 13. The comparison of methods STL1 smooth X and STL2 smooth X highlights the significant effect of the STL pattern. Furthermore, the mesh

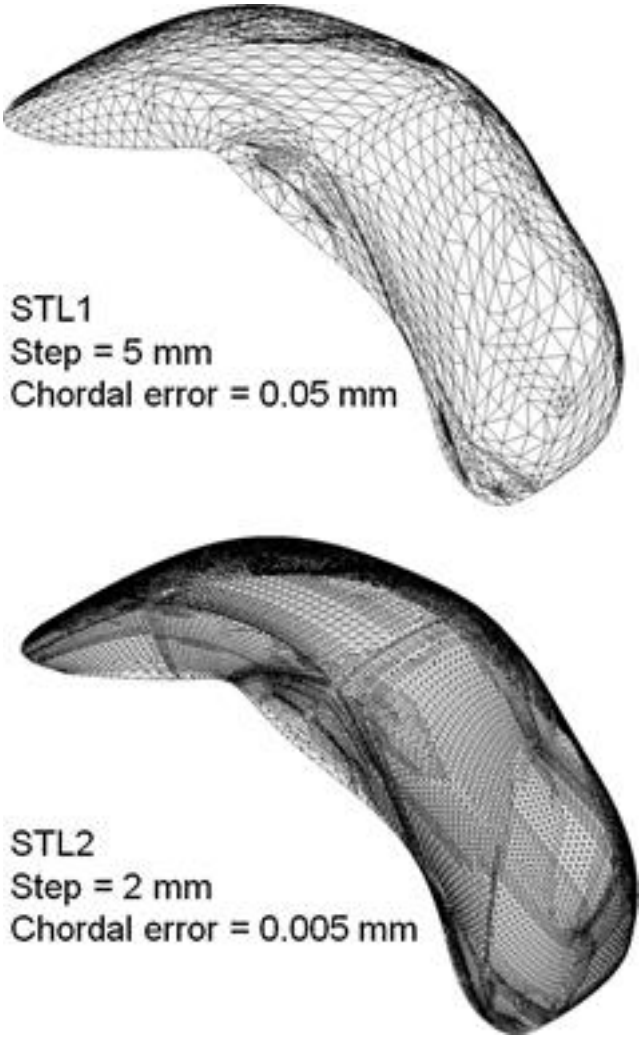


Fig. 14 The STL models 1 and 2

patterns are more emphasized in method STL1 smooth XYZ than in STL1 smooth X.

## 8 Conclusion

This paper presents a method to adapt a toolpath to a geometrical target without recalculating the entire toolpath. The presented application case is to remove a constant thickness on a rough surface. This case is usually present in the production of the femoral component of knee prostheses. The proposed method requires a 3D measure of the rough workpiece. An STL model is usually generated after the measurement process. The toolpath deformation method starts with a best-fit (Iterative Closest Point method) of the measured surface and the toolpath computed on the nominal model. Next, a method to deform the toolpath is proposed. This method can adapt the toolpath to remove a constant thickness on rough surface.

On the other hand, the use of a meshed model to deform the toolpath induces the apparition of pattern marks on the machined surface. To limit this problem, this paper proposes a toolpath smoothing method. This smoothing method is performed to ensure a maximum accepted gap between the toolpath before and after smoothing. This smoothing is based on the use of a polynomial associated with the least square method.

Subsequently, tests are proposed to validate the usefulness of the presented method. A first test is conducted on an industrial surface. It validates the toolpath deformation. Furthermore, this test highlights the faceting of the toolpath (and consequently the machined surface) caused by the STL model. The second test is carried out to validate the usefulness of the smoothing method

Fig. 15 Effects of smoothing strategies and STL refinements

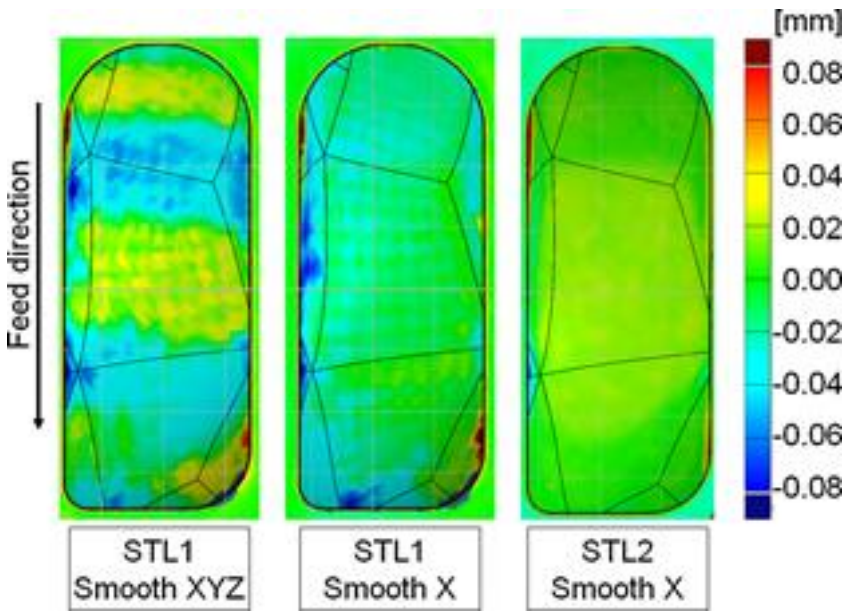

and the effect of STL refinement on the machined surface quality. This test highlights the contribution of the smoothing method and the importance of STL quality.

## References


1. Lison D, Lauwerys R, Demedts M, Nemery B (1996) Experimental research into the pathogenesis of cobalt/hard metal lung disease. European Respiratory Journal 9:1024–1028. doi:10.1183/09031936.96.09051024
2. Chaves-Jacob J, Linares J-M, Sprauel J-M (2013) Improving tool wear and surface covering in polishing via toolpath optimization. Journal Of Materials Processing Technology 213(10):1661–1668. doi:10.1016/j.jmatprotec.2013.04.005
3. Boukebbab S, Bouchenitfa H, Boughouas H, Linares JM (2007) Applied Iterative Closest Point algorithm to automated inspection of gear box tooth. International Journal of Computers & Industrial Engineering 52:162–173. doi:10.1016/j.cie.2006.12.001
4. Besl PJ, Mckay ND (1992) A method for registration of 3-D shapes. IEEE Transactions on Pattern Analysis and Machine Intelligence 14(2):239–256. doi:10.1109/34.121791
5. Zhu L, Barhak J, Srivatsan V, Katz R (2007) Efficient registration for precision inspection of free-form surfaces. International Journal of Advance Manufacturing Technology 32:505–515. doi:10.1007/s00170-005-0370-9
6. Ezra E, Sharir M, Efrat A (2008) On the performance of the ICP algorithm. Computational Geometry 41:77–93. doi:10.1016/j.comgeo.2007.10.007
7. Kim D, Kim D (2010) A fast ICP algorithm for 3-D human body motion tracking. IEEE Signal Process Lett 17:402–405. doi:10.1109/LSP.2009.2039888
8. Ma B, Ellis RE (2003) Robust registration for computer-integrated orthopedic surgery: laboratory validation and clinical experience. Medical Image Analysis 7:237–250. doi:10.1016/S1361-8415(02)00133-0
9. Kaneko S, Kondo T, Miyamoto A (2003) Robust matching of 3D contours using iterative closest point algorithm improved by M-estimation. The Journal of the Pattern Recognition Society 36:2041–2047. doi:10.1016/S0031-3203(03)00050-5
10. Bearee R, Dieulot JY, Rabate P (2011) An innovative subdivision-ICP registration method for tool-path correction applied to deformed aircraft parts machining. International Journal of Advanced Manufacturing Technology 53:463–471. doi:10.1007/s00170-010-2875-0
11. Smith S, Woody B, Ziegert J, Huang Y (2007) Deformation machining—a new hybrid process. Annals of the CIRP 56(1):281–284. doi:10.1016/j.cirp.2007.05.065
12. Redonnet JM, Rubio W, Dessein G (1998) Side milling of ruled surfaces: optimum positioning of the milling cutter and calculation of interference. International Journal of Advanced Manufacturing Technology 14(7):459–465. doi:10.1007/BF01351391
13. Menzel C, Bedi S, Mann S (2004) Triple tangent flank milling of ruled surfaces. Computer Aided Design 36(3):289–296. doi:10.1016/S0010-4485(03)00118-0
14. Belchior J, Guillo M, Courteille E, Maurine P, Leotoing L, Guines D (2013) Off-line compensation of the tool path deviations on robotic machining: application to incremental sheet forming. Robotics and Computer-Integrated Manufacturing 29:58–69. doi:10.1016/j.rcim.2012.10.008
15. Biermann D, Krebs E, Sacharow A, Kersting P (2012) Using NC-path deformation for compensating tool deflections in micromilling of hardened steel. Procedia CIRP 1:132–137. doi:10.1016/j.procir.20 12.04.022
16. Wan X-JH ua L, Wang X-F, Peng Q-Z, Qin X-p (2011) An error control approach to tool path adjustment conforming to the deformation of thin-walled workpiece. International Journal of Machine Tools & Manufacture 51:221–229. doi:10.1016/j.ijmachtools.2010.11.007
17. Bearee R, Dieulot J-Y, Rabate P (2011) An innovative subdivision-ICP registration method for tool-path correction applied to deformed aircraft parts machining. International Journal Of Advanced Manufacturing Technology 53(5–8):463–471. doi:10.1007/s00170-010-2875-0
18. Lartigue C, Tournier C, Ritou M, Dumur D (2004) High-performance NC for HSM by means of polynomial trajectories. CIRP Annals 53(1):317–320. doi:10.1016/S0007-8506(07)60706-9
19. Tournier C, Duc E (2005) Iso-scallop tool path generation in 5-axis milling. International Journal of Advanced Manufacturing Technology 25:867–875. doi:10.1007/s00170-003-2054-7
20. Can A, Unuvar A (2010) Five-axis tool path generation for 3D curves created by projection on B-spline surfaces. International Journal of Advanced Manufacturing Technology 49:1047–1057. doi:10.1007/s00170-009-2459-z